Stochastic Cloning: A generalized framework for processing relative state measurements

Stergios I. Roumeliotis and Joel W. Burdick
Division of Engineering and Applied Science
California Institute of Technology, Pasadena, CA[1]

Abstract

This paper introduces a generalized framework, termed "stochastic cloning," for processing relative state measurements within a Kalman filter estimator. The main motivation and application for this methodology is the problem of fusing displacement measurements with position estimates for mobile robot localization. Previous approaches have ignored the developed interdependencies (cross-correlation terms) between state estimates of the same quantities at different time instants. By directly expressing relative state measurements in terms of previous and current state estimates, the effect of these cross-correlation terms on the estimation process is analyzed and considered during updates. Simulation and experimental results validate this approach.

1 Introduction

In order for a mobile robot to autonomously navigate, it must be able to localize itself [1], i.e. to know its position and orientation (pose). Different types of sensors [2] and techniques have been employed to address this issue (e.g. [3], [4], [5], [6]). Most current localization systems combine measurements from *proprioceptive* sensors that monitor the vehicle's motion with information collected by *exteroceptive* sensors that provide information about the robot's neighboring environment. Examples of proprioceptive sensors include wheel encoders, accelerometers, gyroscopes, etc. By applying appropriate integration of the measured quantities, the robot's displacement can be estimated. However, the integration of noise contaminating these signals, causes the position estimate to drift from its real value [7], [8]. The exteroceptive sensors extract information about the robot's configuration by measuring the unique characteristics of the robot's surroundings. Exteroceptive sensors can also be used to derive direct estimates of a vehicle's motion (motion from structure). For example, laser scan matching and vision based correlation techniques [9, 10, 11, 12] can be employed to estimate a robot's displacement between successive sensor samples. This estimate is computed by minimizing some function of the distance between the corresponding locations within a set of laser scans or image frames where a set of features appear.
Once a displacement measurement is derived from an ex-

teroceptive sensor, in most cases it must be combined with other position estimates derived from onboard proprioceptive sensors. An appealing solution to this problem is to convert the relative pose measurements to absolute position pseudo-measurements using the previous position estimates and treat them as such [13]. A different approach would be to process the displacement information as an (average) velocity measurement during the time interval between consecutive images [14]. Both these methodologies are approximate solutions founded on certain assumptions. The first approach is correct only when the orientation of the vehicle is precisely known. The second approach is valid only when the frequency of the displacement measurements is higher or at least equal to the frequency of any other velocity measurements available to the estimator. If both odometry and the relative pose measurements are available at the same rate, an exact solution would be to combine them as two independent measurements of the same displacement between two consecutive time steps. In most practical situations relative pose measurements are obtained at a significantly lower rate compared to odometric data. Application of this last methodology cannot provide state estimates between relative pose measurements unless two different estimators are involved; one for state estimation (absolute pose) and one for odometry integration.

A more formal approach to this problem is to treat the relative displacement estimates as differences between the previous and current estimates of the position of the robot. In this paper we present a generalized framework, which we term *stochastic cloning*[1] for processing such relative state (pose in this case) measurements within a Kalman filter (KF) estimator. To our knowledge, this paper represents the first thorough investigation of how to fuse such relative displacement measurements with proprioceptive measurements in order to provide improved position estimates.

Section 3 presents the proposed methodology. Section 4 applies this approach to the case of a mobile robot moving on flat terrain. Section 5 presents simulation and experimental results. We derive our conclusions in Section 6, and suggest possible directions of future work.

---

[1]{stergios|jwb}@robotics.caltech.edu.

[1]From the Oxford English Dictionary: [ad. Greek κλών twig, slip], [*clone, v.* To propagate or reproduce (an identical individual) from a given original; to replicate (an existing individual).]

2 Background

We first recall the classical Extended Kalman Filter (EKF) framework, so that we may motivate the need for our stochastic cloning approach. The time evolution of the state of an observed system can generally be described as:

$$\dot{\vec{x}} = f(\vec{x}, \vec{u}, \vec{w}, t) \tag{1}$$

where f is a possibly non-linear time-varying function of the state $\vec{x}(t)$, the control inputs $\vec{u}(t)$ and the unmodeled disturbances (system noise) $\vec{w}(t)$. The analogous equation in discrete time is:

$$\vec{x}(t_{k+1}) = f_{k+1}(\vec{x}(t_k), \vec{u}(t_k), \vec{w}(t_k)) \tag{2}$$

In order to derive the (propagation) equations of a EKF observer that estimates the system state, the previous equations are linearized:

$$\widetilde{\vec{x}}(t_{k+1}) = F_{k+1}\widetilde{\vec{x}}(t_k) + G_{k+1}\vec{w}(t_k) \tag{3}$$

where $\widetilde{\vec{x}}(t_k)$, $\widetilde{\vec{x}}(t_{k+1})$ are the errors in the state estimate before and after the propagation. Assume that measurements $\vec{z}(t_{k+m})$ of the state $\vec{x}(t_{k+m})$ are available at some time t_{k+m}

$$\vec{z}(t_{k+m}) = h_{k+m}(\vec{x}(t_{k+m})) + \vec{v}(t_{k+m}) \tag{4}$$

where h_{k+m} is, in general, a non-linear time-varying function of the *current* state $\vec{x}(t_{k+m})$, and the noise $\vec{v}(t_{k+m})$ associated with this measurement. Linearization of Eq. (4) yields

$$\widetilde{\vec{z}}(t_{k+m}) = H_{k+m}\widetilde{\vec{x}}(t_{k+m}) + \vec{v}(t_{k+m}) \tag{5}$$

where

$$H_{k+m} = \nabla_{\vec{x}_{k+m/k}} h_{k+m}(\widehat{\vec{x}}_{k+m/k}) \tag{6}$$

and $\widetilde{\vec{x}}_{k+m/k}$, $\widetilde{\vec{z}}(t_{k+m})$ are the errors in state estimate and measurement, and $\widehat{\vec{x}}_{k+m/k}$ is an estimate of the state $\vec{x}$ at time $k+m$ given measurements up to time k. The Kalman filter ([15] pg. 217) can be used to compute an updated estimate of the system state $\widehat{\vec{x}}_{k+m/k+m}$ using the (propagated) previous state estimate $\widehat{\vec{x}}_{k+m/k}$ and the current measurement $\vec{z}_{k+m} = \vec{z}(t_{k+m})$. The implicit assumption made here is that the measurements $\vec{z}_{k+m}$ depend only on the *current* state of the system. In cases when the measurement vector reflects *changes* in the state of the system during a certain time interval instead of the state itself, the previous formulation has to be modified. Such modifications are necessary when relative displacement measurements, as the ones produced by range scan matching algorithms, must be processed.

3 Approach

Often, proprioceptive measurements, necessary to propagate the state estimates, will be available at each integer time step, while relative state measurements will occur at some lower rate, say every m time steps. If the measured quantities depend on the current $\vec{x}(t_{k+m})$ as well as the previous $\vec{x}(t_k)$ state of the system then the measurement equation is:

$$\vec{z}(t_{k+m}) = h_{k+m/k}(\vec{x}(t_{k+m}), \vec{x}(t_k)) + \vec{v}(t_{k+m}) \tag{7}$$

In this case the error in this measurement will depend on both previous and current state of the system and therefore Eq. (5) must be written as:

$$\widetilde{\vec{z}}(t_{k+m}) = H_{k+m/k}\widetilde{\vec{x}}_{k+m/k} + H_{k/k}\widetilde{\vec{x}}_{k/k} + \vec{v}(t_{k+m}) \tag{8}$$

where

$$\begin{aligned} H_{k+m/k} &= \nabla_{\vec{x}_{k+m/k}} h_{k+m/k}(\widehat{\vec{x}}_{k+m/k}) \\ H_{k/k} &= \nabla_{\vec{x}_{k/k}} h_{k/k}(\widehat{\vec{x}}_{k/k}) \end{aligned} \tag{9}$$

and $\widetilde{\vec{x}}_{k/k}$, $\widetilde{\vec{x}}_{k+m/k}$, are the errors in the previous and current estimates and $\widetilde{\vec{z}}(t_{k+m})$ is the measurement error. As evident from Eqs. (8), (9), the previous state estimate $\widehat{\vec{x}}_{k/k}$ is necessary in order to evaluate the current measurement uncertainty. Even though, based on the Markovian assumption, all the information from previous estimates is included in the current state estimate and both the previous state $\widehat{\vec{x}}_{k/k}$ and covariance $P_{k/k}$ (with $P_{k/k} = E\{\widehat{\vec{x}}_{k/k}\, \widehat{\vec{x}}_{k/k}{}^T\}$) estimates are available, there is no direct way in the classical EKF framework to determine the cross-correlation between the current and the previous state estimates.

In order to appropriately derive the interdependencies between estimates of the state at different time instants, we augment the state of the Kalman filter to include two identical copies of the state estimate—hence the name stochastic cloning. At time t_k the state vector for the augmented system is:

$$\breve{\vec{x}}(t_k) = \begin{bmatrix} \widetilde{\vec{x}}(t_k)_s \\ \widetilde{\vec{x}}(t_k) \end{bmatrix} \tag{10}$$

where $\widetilde{\vec{x}}(t_k)_s$ and $\widetilde{\vec{x}}(t_k)$ are the stationary and evolving clone of the same state vector at time t_k. The first state corresponds to the system state with respect to which the relative state measurement (e.g., displacement estimate) was derived. This clone does not evolve any further with time (it is a static quantity) while the second state is propagated according to the time evolution equations of the system described in Eqs. (1) and (2). We now summarize the EKF for the stochastic cloned system.

3.1 Propagation

Since these two estimates in Eq. (10) are identical at time t_k, the covariance matrix for the augmented system will be:

$$\breve{P}_{k/k} = \begin{bmatrix} P_{k/k} & P_{k/k} \\ P_{k/k} & P_{k/k} \end{bmatrix} \tag{11}$$

where $P_{k/k}$ is the covariance of the original (uncloned) system at time t_k. Eq. (3) for the augmented KF will be:

$$\begin{bmatrix} \widetilde{x}(t_{k+1})_s \\ \widetilde{x}(t_{k+1}) \end{bmatrix} = \begin{bmatrix} I & 0 \\ 0 & F_{k+1} \end{bmatrix} \begin{bmatrix} \widetilde{x}(t_k)_s \\ \widetilde{x}(t_k) \end{bmatrix} + \begin{bmatrix} 0 \\ G_{k+1} \end{bmatrix} \vec{w}(t_k)$$

or

$$\breve{x}(t_{k+1}) = \breve{F}_{k+1}\breve{x}(t_k) + \breve{G}_{k+1}\vec{w}(t_k) \qquad (12)$$

The covariance of the augmented system is propagated as:

$$\breve{P}_{k+1/k} = \breve{F}_{k+1}\breve{P}_{k/k}\breve{F}^T_{k+1} + \breve{G}_{k+1}Q_k\breve{G}^T_{k+1} \qquad (13)$$

and after m steps is:

$$\breve{P}_{k+m/k} = \begin{bmatrix} P_{kk} & P_{kk}\mathcal{F}^T \\ \mathcal{F}P_{kk} & P_{k+m/k} \end{bmatrix} \qquad (14)$$

where $\mathcal{F} = \prod_{i=1}^{m} F_{k+i}$, and $P_{k+m/k}$ is the propagated covariance of the evolving state at time t_{k+m}.

3.2 Update

When the relative state measurement is acquired, the covariance matrix for the residual is given by:

$$\breve{S} = \breve{H}\breve{P}_{k+m/k}\breve{H}^T + R_r \qquad (15)$$

where R_r is the covariance of the relative state measurement and

$$\breve{H} = \begin{bmatrix} H_{k/k} & H_{k+m/k} \end{bmatrix} \qquad (16)$$

For example, in [9, 10], R_r is constructed as a by-product of the relative displacement measurement obtained from matching laser range scans. By substituting from Eqs. (14), (16) in Eq. (15) we have:

$$\begin{aligned} \breve{S} = \ & R_r + H_{k/k}P_{k/k}H^T_{k/k} + H_{k+m/k}\mathcal{F}P_{k/k}H^T_{k/k} \qquad (17) \\ & + H_{k/k}P_{k/k}\mathcal{F}H^T_{k+m/k} + H_{k+m/k}P_{k+m/k}H^T_{k+m/k} \end{aligned}$$

The updated covariance matrix for the augmented system is computed by:

$$\breve{P}_{k+m/k+m} = \breve{P}_{k+m/k} - \breve{P}_{k+m/k}\breve{H}^T \breve{S}^{-1}\breve{H}\breve{P}_{k+m/k} \qquad (18)$$

$$= \breve{P}_{k+m/k} - \begin{bmatrix} P_{kk}H^T_{k/k} + P_{kk}\mathcal{F}^T H^T_{k+m/k} \\ \mathcal{F}P_{kk}H^T_{k/k} + P_{k+m/k}H^T_{k+m/k} \end{bmatrix} \breve{S}^{-1} \times$$

$$\begin{bmatrix} H_{k/k}P_{kk} + H_{k+m/k}\mathcal{F}P_{kk} & H_{k/k}P_{kk}\mathcal{F}^T + H_{k+m/k}P_{k+m/k} \end{bmatrix}$$

while the covariance of the evolving state at time t_{k+m} is (lower-right diagonal submatrix):

$$\begin{aligned} P_{k+m/k+m} = \ & P_{k+m/k} - (\mathcal{F}P_{kk}H^T_{k/k} + P_{k+m/k}H^T_{k+m/k})\breve{S}^{-1} \times \\ & (H_{k/k}P_{kk}\mathcal{F}^T + H_{k+m/k}P_{k+m/k}) \end{aligned}$$

The Kalman gain is calculated by:

$$\breve{K} = \begin{bmatrix} K_s \\ K \end{bmatrix} = \breve{P}_{k+m/k}\breve{H}^T\breve{S}^{-1} \qquad (19)$$

with

$$K = (\mathcal{F}P_{k/k}H^T_{k/k} + P_{k+m/k}H^T_{k+m/k})\breve{S}^{-1} \qquad (20)$$

Finally, the updated augmented state is:

$$\breve{x}_{k+m/k+m} = \breve{x}_{k+m/k} + \breve{K}r_{k+m} \qquad (21)$$

where $r_{k+m} = z(t_{k+m}) - \widehat{z}_{k+m}$ is the measurement residual and

$$\widehat{x}_{k+m/k+m} = \widehat{x}_{k+m/k} + Kr_{k+m} \qquad (22)$$

is the updated estimate of the evolving state.

4 Example: Fusion of Odometry and Weighted Laser Scan Matching

This section presents the equations of the modified Kalman filter (SC-KF) that fuses odometric data with relative 2D pose measurements. We apply the equations to both simulated and real data. Our experiments use a particular weighted laser scan matching (WLSM) algorithm [10] to estimate the robot's displacement between two locations via the matching of two consecutive laser scans. However, any algorithm (such as [9]) that estimates relative displacement and yields an estimate of R_r is suitable.

4.1 Propagation

First we describe the propagation equations for the KF using the velocity measurements from the odometric sensors. The estimated state vector consists of the robot's pose with respect to a fixed reference frame: $\vec{x} = [x \ y \ \phi]^T$. For the vehicle's odometry, we use a generic set of equations. However, the method can be easily adapted to a specific vehicle. The continuous time equations for the motion expressed in local coordinates are:

$$^L\dot{x} = V, \ ^L\dot{y} = 0, \ \dot{\phi} = \omega \qquad (23)$$

where V and ω are the linear and angular velocity of the robot as measured by the wheel-encoders' signals. Based on Eq. (23), the linearized discrete-time error-state propagation equation in global coordinates is:

$$\begin{bmatrix} \widetilde{x} \\ \widetilde{y} \\ \widetilde{\phi} \end{bmatrix}_{t_{k+1}} = \begin{bmatrix} 1 & 0 & -V\delta t \sin\phi \\ 0 & 1 & V\delta t \cos\phi \\ 0 & 0 & 1 \end{bmatrix} \begin{bmatrix} \widetilde{x} \\ \widetilde{y} \\ \widetilde{\phi} \end{bmatrix}_{t_k}$$

$$+ \begin{bmatrix} \delta t \cos\phi & 0 \\ \delta t \sin\phi & 0 \\ 0 & \delta t \end{bmatrix} \begin{bmatrix} n_V \\ n_\omega \end{bmatrix} \qquad (24)$$

or

$$\widetilde{x}(t_{k+1}) = F_{k+1}\widetilde{x}(t_k) + G_{k+1}\vec{w}(t_k) \qquad (25)$$

where $\delta t = t_{k+1} - t_k$ and $\vec{w} = \begin{bmatrix} n_V^T & n_\omega \end{bmatrix}^T$ is the system noise due to the errors in the linear and rotational velocity measurements with covariance $Q_k = E\{\vec{w}\vec{w}^T\}$. The covariance propagation equation for this system is obtained by direct application of Eq. (13).

4.2 Relative Pose Measurements

In what follows, we assume that at time t_k the vehicle is at position $^G\vec{p}(t_k) = \ ^G\vec{p}_1$ with orientation $^G\phi(t_k) = \ ^G\phi_1$ and after m steps it has moved to position $^G\vec{p}(t_{k+m}) = \ ^G\vec{p}_2$ with orientation $^G\phi(t_{k+m}) = \ ^G\phi_2$. Frames $\{G\}$, $\{1\}$, and $\{2\}$ are the inertial frames of reference attached to the vehicle at times t_0, t_k and t_{k+m} correspondingly.

If the robot registers two consecutive laser scans at locations $^G\vec{x}_1$ and $^G\vec{x}_2$, the displacement measurement from the WLSM algorithm is:

$$z = \ ^1\vec{x}_2 + \vec{v} = \begin{bmatrix} ^1\vec{p}_2 \\ ^1\phi_2 \end{bmatrix} + \vec{v} = \begin{bmatrix} ^1\vec{p}_2 - \ ^1\vec{p}_1 \\ ^1\phi_2 - \ ^1\phi_1 \end{bmatrix} + \vec{v} =$$

$$\begin{bmatrix} ^G_1C^T(\phi_1)(^G\vec{p}_2 - \ ^G\vec{p}_1) \\ ^G\phi_2 - \ ^G\phi_1 \end{bmatrix} + \vec{v} = \Gamma(^G\vec{x}_2 - \ ^G\vec{x}_1) + \vec{v} \ (26)$$

where $\vec{v}$ is the relative pose measurement noise assumed to be a zero-mean white Gaussian process with covariance $R_r = E\{\vec{v}\vec{v}^T\}$ and

$$\Gamma = \begin{bmatrix} {}_1^G C^T(\phi_1) & 0_{2\times 1} \\ 0_{2\times 1}^T & 1 \end{bmatrix} , \quad C(\phi) = \begin{bmatrix} \cos\phi & -\sin\phi \\ \sin\phi & \cos\phi \end{bmatrix}$$

In the previous equation, the measurement vector is expressed in terms of both corresponding poses of the robot when the two laser scans were recorded. As aforementioned, in order to compute the dependence of the relative pose measurement on the accuracy of the pose estimates at times t_k and t_{k+m} we have to augment the state vector so as to contain both states ${}^G\vec{x}(t_k) = {}^G\vec{x}_1$ and ${}^G\vec{x}(t_{k+m}) = {}^G\vec{x}_2$. The measurement matrix would be

$$\breve{H} = [H_{k/k} \quad H_{k+m/k}] = [\nabla_{\vec{x}_1}\vec{z} \quad \nabla_{\vec{x}_2}\vec{z}] = \Gamma[-D \quad I] \ (27)$$

where

$$D = \begin{bmatrix} I_{2\times 2} & J\ {}^G\Delta\vec{p}_{1,2} \\ 0_{2\times 1}^T & 1 \end{bmatrix} , \quad J = \begin{bmatrix} 0 & -1 \\ 1 & 0 \end{bmatrix}$$

and ${}^G\Delta\vec{p}_{1,2} = {}^G\vec{p}_2 - {}^G\vec{p}_1$.

4.3 State Interdependencies

We now carefully account for the state estimate interdependencies for the case that the state vector contains only the pose of the robot $\vec{x} = [x\ y\ \phi]^T$. The displacement measurement conveys information regarding the pose of the robot at time t_{k+m} with respect to the pose at some previous time t_k. Since the displacement measurement provides *no* new information about the previous state $\vec{x}(t_k)$ (pose of the robot), the uncertainty of its estimate at t_k will not be reduced and therefore the corresponding covariance matrix (the upper-left diagonal submatrix of $\breve{P}_{k+m/k+m}$ in Eq. (18)) must remain the same. In order for this to hold true for every selection of matrices $\breve{S}$ and P_{kk}:[2]

$$H_{k/k} + H_{k+m/k}\mathcal{F} = (H_{k/k}^T + \mathcal{F}^T H_{k+m/k}^T)^T = 0$$

or

$$H_{k/k} = -H_{k+m/k}\mathcal{F} \quad (28)$$

By substituting Eq. (28) in Eq. (8) the estimated (expected) measurement error is:

$$\widetilde{z}(t_{k+m}) = H_{k+m/k}(\widetilde{\vec{x}}_{k+m/k} - \mathcal{F}\widetilde{\vec{x}}_{k/k}) + \vec{v}(t_{k+m}) \quad (29)$$

where $\widetilde{\vec{x}}_{k+m/k}$ is the expected error in the current pose and $\mathcal{F}\widetilde{\vec{x}}_{k/k}$ is the expected error in the pose of the robot at time t_k propagated to time t_{k+m}. We have proven the following:

Lemma 1 *The error in the relative state measurement of the current system state - containing only pose estimates - at time t_{k+m} with respect to a previous state at time t_k is proportional to the difference between the current error in the system state at t_{k+m} and the previous error at time t_k, propagated to time t_{k+m}.*

---

[2]For this 2-dimensional example case, by substituting F_{k+1} from Eq. (24) in $\mathcal{F} = \prod_{i=1}^m F_{k+i}$ it can be shown that $D = \mathcal{F}$ and therefore Eq. (28) is satisfied.

The following remarks clarify the properties and effects of the interdependencies.

Note 1: In practice, Eq. (28) may *not* always hold true for all matrices $H_{k/k}$ and $-H_{k+m/k}\mathcal{F}$ because of the linear approximations required to derive the measurement matrix $\breve{H}$ in Eq. (27). Nevertheless, Eq. (28) has to be enforced otherwise the relative pose measurement update will affect the estimates at time t_k even though no absolute state measurement became available between t_k and t_{k+m}.

Substituting Eq. (28) in Eq. (18), the updated covariance matrix for the new system state will be (lower-right diagonal submatrix):

$$P_{k+m/k+m} = P_{k+m/k} - (P_{k+m/k} - \mathcal{F}P_{kk}\mathcal{F}^T)H_{k+m/k}^T$$
$$\times \breve{S}^{-1}H_{k+m/k}(P_{k+m/k} - \mathcal{F}P_{kk}\mathcal{F}^T) \ (30)$$

where the covariance of the residual from Eq. (17) is now written as:

$$\breve{S} = H_{k+m/k}(P_{k+m/k} - \mathcal{F}P_{k/k}\mathcal{F}^T)H_{k+m/k}^T + R_r \quad (31)$$

Note 2: Note that $\breve{S}$ is a positive definite matrix. From Eq. (13):

$$P_{k+m/k} = (\prod_{i=1}^m F_{k+i})P_{k/k}(\prod_{i=1}^m F_{k+i})^T$$
$$+ \sum_{i=0}^m ((\prod_{j=0}^i F_{k+j})G_{k+i}Q_{k+i}G_{k+i}^T(\prod_{j=0}^i F_{k+j})^T)$$

or

$$P_{k+m/k} = \mathcal{F}P_{k/k}\mathcal{F}^T + \Delta P_{k,k+m}^{(-)} \quad (32)$$

where $\Delta P_{k,k+m}^{(-)}$ is a positive definite matrix which corresponds to the influx of uncertainty in the system during the time interval $[t_k\ t_{k+m}]$. Therefore $\breve{S}$ in Eq. (31) is also a positive definite matrix.

Note 3: By subtracting $\mathcal{F}P_{k/k}\mathcal{F}^T$ from both sides of Eq. (30), and reducing the results, one obtains:

$$P_{k+m/k+m} = \mathcal{F}P_{k/k}\mathcal{F}^T + \Delta P_{k,k+m}^{(+)} \quad (33)$$

where $\Delta P_{k,k+m}^{(+)}$ is the covariance matrix that corresponds to the influx of uncertainty in the system during the time interval $[t_k, t_{k+m}]$, after it has been updated using the relative state measurement. By invoking the matrix inversion lemma:

$$\Delta P_{k,k+m}^{(+)^{-1}} = \Delta P_{k,k+m}^{(-)^{-1}} + H_{k+m/k}^T R_r^{-1} H_{k+m/k}$$

This last relation expresses the fact that the information available to the system between t_k and t_{k+m} is increased by the projection of the information pertinent to the system due to the relative state measurement.[3] Finally, Eq.

---

[3]Note also that the influx of uncertainty $\Delta P_{k,k+m}^{(-)}$ during $[t_k, t_{k+m}]$ is reduced to $\Delta P_{k,k+m}^{(+)}$ which is lower that either of $\Delta P_{k,k+m}^{(-)}$ or $H_{k+m/k}^T R_r^{-1} H_{k+m/k}$.

(33) denotes that the uncertainty after the update at t_{k+m} is equal to the uncertainty at t_k propagated to time t_{k+m} and increased by the *updated* influx of uncertainty during this time interval.

4.4 Update equations

The equations for the residual covariance, state covariance update, and Kalman gain are obtained from Eqs. (31), (30), and (20) respectively, by direct substitution from Eqs. (27), (28):

$$\check{S} = \Gamma(P_{k+m/k} - \mathcal{F}P_{k/k}\mathcal{F}^T)\Gamma^T + R_r \qquad (34)$$

where by multiplying both sides of the previous equation with $\Gamma^T = \Gamma^{-1}$ we define $\widetilde{S}$ as the covariance of the pseudo-residual $\widetilde{r}_{k+m} = \Gamma^T r_{k+m}$ expressed in global coordinates:

$$\widetilde{S} = P_{k+m/k} - \mathcal{F}P_{k/k}\mathcal{F}^T + \widetilde{R}_r \qquad (35)$$

with $\widetilde{R}_r = \Gamma^T R_r \Gamma$,

$$P_{k+m/k+m} = P_{k+m/k} - (P_{k+m/k} - \mathcal{F}P_{kk}\mathcal{F}^T)$$
$$\times \widetilde{S}^{-1}(P_{k+m/k} - \mathcal{F}P_{kk}\mathcal{F}^T) \qquad (36)$$

and

$$K = (P_{k+m/k} - \mathcal{F}P_{k/k}\mathcal{F}^T)\widetilde{S}^{-1}\Gamma^T = \widetilde{K}\Gamma^T \qquad (37)$$

The upper submatrix of the Kalman gain matrix in Eq. (19) is zero, as expected (no correction takes place regarding the previous pose estimate). The pseudo-residual is:

$$\widetilde{r}_{k+m} = \Gamma^T r_{k+m} = \Gamma^T \left(z(t_{k+m}) - \Gamma \begin{bmatrix} {}^G\Delta\hat{p}_{1,2} \\ {}^G\Delta\hat{\phi}_{1,2} \end{bmatrix} \right)$$
$$= \Gamma^T z(t_{k+m}) - \left(\hat{\widetilde{x}}_{k+m/k} - \hat{\widetilde{x}}_{k/k} \right) \qquad (38)$$

Finally, the updated pose estimate is given by:

$$\hat{\widetilde{x}}_{k+m/k+m} = \hat{\widetilde{x}}_{k+m/k} + K r_{k+m}$$
$$= \hat{\widetilde{x}}_{k+m/k} + \widetilde{K}\widetilde{r}_{k+m}$$
$$= (I - \widetilde{K})\hat{\widetilde{x}}_{k+m/k} + \widetilde{K}(\hat{\widetilde{x}}_{k/k} + \Gamma^T z(t_{k+m}))$$
$$= (I - \widetilde{K})\hat{\widetilde{x}}_{k+m/k} + \widetilde{K}\bar{x}_{k+m} \qquad (39)$$

From this last equation it is evident that the updated pose estimate $\hat{\widetilde{x}}_{k+m/k+m}$ at time t_{k+m} is the weighted average of the propagated (through odometry) pose estimate $\hat{\widetilde{x}}_{k+m/k}$ and the absolute pose pseudo-measurement $\bar{x}_{k+m}$ which is computed by appropriately combining the pose estimate $\hat{\widetilde{x}}_{k/k}$ at time t_k with the relative pose measurement $z(t_{k+m})$.

The same process is repeated every time a new relative pose measurement $z(t_{k+m_i})$ becomes available. The previous treatment makes the assumption that the measurements $z(t_{k+m_i})$ are independent, i.e. $E\{z(t_{k+m_i})z^T(t_{k+m_j})\} = 0$. If the WLSM algorithm uses the same set of features from an intermediate laser scan
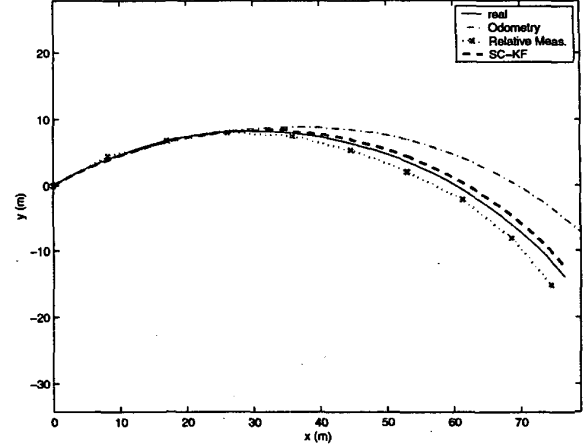
to track the pose of the vehicle through two consecutive steps then these measurements are loosely correlated:

$$E\{z(t_{k+m_i})z^T(t_{k+m_{i+1}})\} \neq 0$$
$$E\{z(t_{k+m_i})z^T(t_{k+m_{i+1}})\} << E\{z(t_{k+m_i})z^T(t_{k+m_i})\}$$

In this case the correlations have to be explicitly addressed by the estimation algorithm. The interested reader is referred to [16] for a detailed treatment of this case.
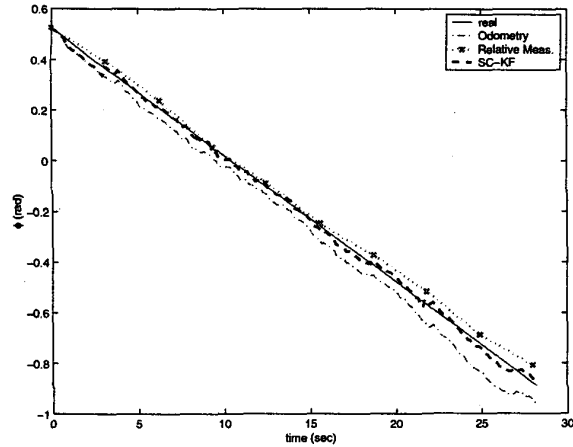
5 Results

5.1 Simulation results

Figure 1: Trajectory $(x-y)$: The solid line represents the real path, the dashed-dotted (-.) line is the deadreckoned path computed by integrating the odometric data, the dotted (:) line is the path calculated by combining the relative pose measurements (x), and the dashed (–) line is the estimated path by the SC-KF.

We first tested the SC variant of the Kalman filter in simulation. As it was described before, during most of the time the pose estimate of the robot is propagated using odometric data (linear and rotational velocity measurements). Since relative pose measurements are available at a lower rate, updates occur only intermittently (here every 3 sec). Three different estimates were considered for comparison purposes: (i) the deadreckoned estimates, computed by integrating the odometric data, (ii) the pose estimates by combining the successive (intermittent) displacement measurements, and (iii) the estimates from the SC-KF that fuses odometric data with the relative state information. As it will be evident from the results presented here, the SC-KF estimates are, on the average, of higher accuracy compared to those from any of the other two methods. In addition, the rate of increase of the estimation uncertainty due to the odometric or relative pose measurement errors is significantly reduced when these are combined within the SC-KF.

An example trajectory is shown in Fig. 1. At the beginning the odometry data are trusted more by the filter
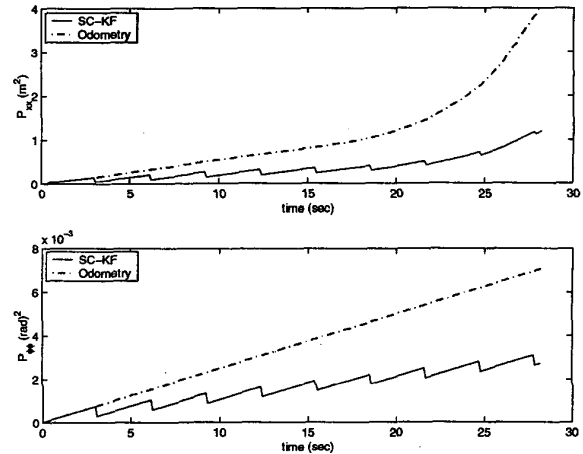
Figure 2: Orientation estimates: The solid line represents the real values of ϕ, the dashed-dotted (-.) depicts the deadreckoned estimates computed by integrating the odometric data, the dotted (:) line is calculated by combining the relative pose measurements (x), and the dashed (-) line represents the estimates by the SC-KF.

Figure 3: (a) Covariance of x computed by dead-reckoning (dashed-dotted line) and the SC-KF (solid line). (b) Covariance of ϕ computed by dead-reckoning (dashed-dotted line) and the SC-KF (solid line).

while later on the SC-KF values more the relative displacement information. Fig. 2 presents the corresponding orientation estimates during the same time. For the simulation results presented here the relative pose measurements had accuracy $\pm 4.5°$ for the orientation and $\pm 0.8m$ for the position for every 9 meters of actual displacement. The standard deviation for the odometric noise components was $\sigma_V = 0.5(m/sec)/\sqrt{(Hz)}$ for the linear velocity and $\sigma_\omega = 3(°/sec)/\sqrt{(Hz)}$ for the rotational velocity. Note that during every time interval bounded by two consecutive relative pose measurements, the filter relies solely on the odometric information in order to propagate the state estimates. Therefore the influx of uncertainty inbetween the intermittent updates is the same as that during dead-reckoning.

This is evident in Fig. 3 which depicts the time evolution of the covariances for the x and ϕ estimates. When only odometric data are considered (dead-reckoning), the uncertainty for these estimates grows monotonically reflecting the deterioration in positioning accuracy. By appropriately incorporating relative pose information, the SC-KF in effect reduces the estimation uncertainty every time a displacement measurement becomes available. The result of processing this additional positioning information, within the SC-KF, manifests itself as a saw-tooth pattern in the covariance estimates (Fig. 3). The magnitude of the intermittent covariance reductions is determined by the quality of the relative pose measurements.

The orientation uncertainty depends only on the orientation information available to the SC-KF. Therefore (Fig. 3-b), the rate of increase (slope) of the orientation covariance, in the SC-KF, between two updates is exactly the

same as in dead-reckoning. This is not the case for the position covariance (Fig. 3-a). The position uncertainty depends on both the available positioning information and on the quality of the previous and current orientation estimates. Thus, right after every relative pose measurement not only the magnitude of the positioning uncertainty is reduced, but also the rate of increase of the position covariance is lower compared to the corresponding interval of dead-reckoning. This is due to the fact that the updated orientation estimates allow for increased accuracy in the position estimates.

Statistical evaluation of the SC-KF based on simulation results from 100 trials are presented in Fig. 4. These plots depict the standard deviation of the errors in position x, y and orientation ϕ during 10 consecutive updates. As before, 30 steps of propagation (not shown in this figure) were encountered between these updates. The standard deviation of the odometric errors had similar values with those of the estimation errors when only relative pose measurements were processed to compute the pose of the robot. The SC-KF estimation errors are lower compared to either odometry or relative pose data. In particular for the orientation, the standard deviation for the SC-KF is $\sigma_{SC-KF}^{-1} = \sigma_{odom.}^{-1} + \sigma_{rel.\ meas.}^{-1}$ as two independent sources of information are linearly combined within the filter.

Finally, as evident from Figs. 3, 4, the covariance of the pose estimates even within the SC-KF will continue to grow, albeit at a lower rate. Absolute positioning information is necessary periodically in order to limit the maximum uncertainty in the system. Nevertheless, by reducing the rate of covariance increase, the SC-KF is able to extend the period that the robot can operate within acceptable levels of uncertainty before a global update is required.
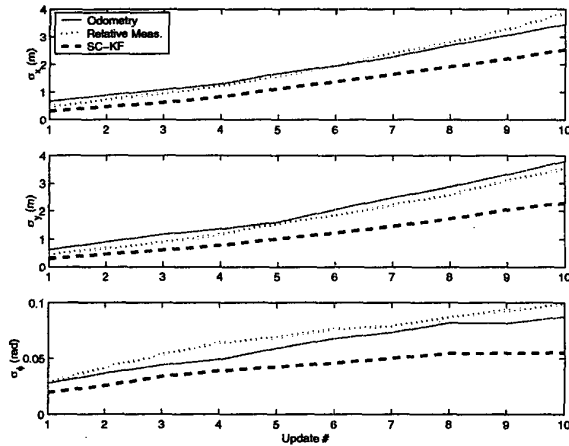
Figure 4: Monte Carlo simulation tests (100 runs): Standard deviation of the errors in x, y, and ϕ during 10 consecutive updates.

5.2 Experimental results

Location	Odometry	WLSM	SC-KF
2	12	5	11
3	28	45	26
4	34	79	52
5	22	114	82
6	44	138	100
7	107	183	139
8	150	174	133
9	216	173	138
10	161	90	57
11	226	37	12
12	367	17	34
13	542	54	66
14	758	95	102
15	951	125	127
Avg.	258.5	94.9	77.0

Table 1: Position errors: Distance between estimated and actual position (in mm).

In order to validate the SC-KF experimentally we fused odometry data from a Nomad 200 mobile robot with the relative displacement measurements from the Weighted Laser Scan Matching (WLSM) algorithm described in detail in [10].

The robot moved between 15 designated locations following 14 consecutive straight-line segments in a closed loop path that brought it to the same starting position (Fig. 5). At each location the robot stopped and rotated its upper portion allowing the laser sensor to measure distances to the surroundings at increments of 0.5° from a 360° field of view. The WLSM algorithm incorporates detailed models of the various sources of noise and uncertainty in the laser scanner data and computes estimates of the position
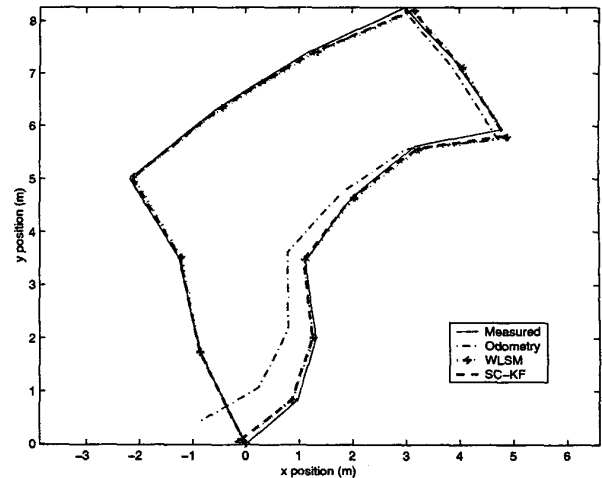

Figure 5: Trajectory $(x - y)$: The solid line connects the reference points that the robot went through. The coordinates of these locations were measured manually. The dashed-dotted (-.) line connects the deadreckoned positions computed by integrating the odometric data, the dotted (:) line connects the positions calculated by combining the relative pose measurements (+), and the dashed line (- -) connects the positions estimated by the SC-KF.

and orientation displacement of the robot as well as the covariance matrices associated with these estimates.

In the path depicted in Fig. 5, the robot traveled a total distance of 22.25 meters. The SC-KF tracks the position of the robot using odometric data and provides updates every time a relative pose measurement becomes available. Three different estimates were computed for comparison purposes: (i) Odometry, (ii) WLSM estimates, and (iii) SC-KF estimates. The actual position of the robot was measured manually and the errors in the position estimates from the three different estimation processes are capsulated in Table 1. These errors are computed as the distance (in mm) between the estimated and the actual position of the robot at 14 locations along its path.

As evident from Table 1, the errors in the position estimates computed by the SC-KF were on average (last row) smaller compared to either the errors in the corresponding odometry estimates, or the errors in the position estimates derived by directly combining the relative displacements. This increased accuracy results from the optimal fusion of two independent sources of information within the SC-KF.

6 Extensions and Future Work

In this paper we presented a generalized framework for processing relative state measurements within a Kalman filter estimator. We derived the equations for the SC-KF when two state estimates, corresponding to different time

instants, had to be considered for estimating the errors in the relative state measurements. The same methodology can be extended to describe the time-correlation between any number of states that a relative state measurement depends on.

The motivation and application for this new approach was the problem of mobile robot localization. We showed that the SC-KF is optimally combining odometric data (from wheel encoders) with relative displacement measurements computed by the WLSM algorithm. The SC-KF can also be modified to fuse other forms of kinetic information, such as linear accelerations and angular velocities measured by an IMU, with a combination of relative position and attitude measurements from a variety of sensing modalities (e.g. vision-based feature tracking [12, 11], laser scan matching [9, 10], etc).

Another potential application for the SC-KF is to incorporate measurements of (higher order) states that are not estimated within the filter. For example, since the Indirect form of the Kalman filter, commonly used in inertial navigation [15, 17], is based on sensor modeling and processes directly linear accelerations and angular velocities measured by an IMU, the errors in these quantities do not appear in the state vector. Therefore there is no clear way to incorporate additional measurements of rotational velocity and linear acceleration into the filter. An example would be the case when the rotational velocity of a vehicle can be calculated from the signals of the encoders attached on its wheels. These measurements can be transformed (through integration) to relative orientation measurements and processed as such by exploiting the stochastic cloning-based variant of the Kalman filter. Finally, as we described in Section 5, the relative pose measurements are usually available at a lower frequency than the kinetic (from the encoders) measurements and produce sharp decreases in the uncertainty of the estimates (especially for the orientation). This reduction in uncertainty incurring at time t_{k+m} can be back-propagated to all time instants between t_k and t_{k+m} by employing a smoother [5]. Improved attitude estimates throughout this time interval will also improve the position estimates. This is within the scope of our future work.

Acknowledgments

References

[1]   I. J. Cox, "Blanche-An experiment in guidance and navigation of an autonomous robot vehicle," *IEEE Transactions on Robotics and Automation*, vol. 7, no. 2, pp. 193–204, April 1991.

[2]   H. R. Everett, *Sensors for Mobile Robots*, AK Peters, 1995.

[3]   J. J. Leonard and H. F. Durrant-Whyte, "Mobile robot localization by tracking geometric beacons," *IEEE Transactions on Robotics and Automation*, vol. 7, no. 3, pp. 376–382, June 1991.

[4]   J. Neira, J. Tardos, J. Horn, and G. Schmidt, "Fusing range and intensity images for mobile robot localization," *IEEE Transactions on Robotics and Automation*, vol. 15, no. 1, pp. 76–84, Feb. 1999.

[5]   S. I. Roumeliotis, G. S. Sukhatme, and G. A. Bekey, "Smoother-based 3-D attitude estimation for mobile robot localization," in *Proceedings of the IEEE International Conference on Robotics and Automation*, Detroit, MI, May 10-15 1999, vol. 3, pp. 1979–1986.

[6]   N. Vlassis, Y. Motomura, and B. Krose, "Supervised dimension reduction of intrinsically low-dimensional data," *Neural Computation*, vol. 14, no. 1, pp. 191–215, Jan. 2002.

[7]   Y. Fuke and E. Krotkov, "Dead reckoning for a lunar rover on uneven terrain," in *Proceedings of the IEEE International Conference on Robotics and Automation*, 1996, pp. 411–416.

[8]   B. Barshan and H. F. Durrant-Whyte, "Inertial navigation systems for mobile robots," *IEEE Trans. on Robotics and Automation*, vol. 11, no. 3, pp. 328–342, June 1995.

[9]   F. Lu and E. Milios, "Robot pose estimation in unknown environments by matching 2d range scans," *Journal of Intelligent and Robotic Systems: Theory and Applications*, vol. 18, no. 3, pp. 249–275, March 1997.

[10]   S. T. Pfister, K. L. Kriechbaum, S. I. Roumeliotis, and J. W. Burdick, "Weighted range sensor matching algorithms for mobile robot displacement estimation," in *Proceedings of the IEEE International Conference on Robotics and Automation*, Washington D.C., May 11-15 2002.

[11]   A. E. Johnson and L. H. Matthies, "Precise image-based motion estimation for autonomous small body exploration," in *Proc. 5th Int'l Symp. On Artificial Intelligence, Robotics and Automation in Space*, June 1999, pp. 627–634.

[12]   C. F. Olson and L. H. Matthies, "Maximum likelihood rover localization by matching range maps.," in *Proceedings of the IEEE International Conference on Robotics and Automation*, Leuven, Belgium, 16-20 May 1998, pp. 272–277.

[13]   B. D. Hoffman, E. T. Baumgartner, T. L. Huntsberger, and P. S. Shenker, "Improved state estimation in challenging terrain," *Autonomous Robots*, vol. 6, no. 2, pp. 113–130, April 1999.

[14]   S. I. Roumeliotis, "A Kalman filter for processing 3-D relative pose measurements," Tech. Rep., Robotics Laboratory, California Institute of Technology, Sep. 2001, http://robotics.caltech.edu/~stergios/tech_reports/relative_3d_kf.pdf.

[15]   P. S. Maybeck, *Stochastic Models, Estimation and Control*, vol. 141-1 of *Mathematics in Science and Engineering*, Academic Press, 1979.

[16]   S. I. Roumeliotis, "Treatment of correlations in relative pose measurements," Tech. Rep., Robotics Laboratory, California Institute of Technology, March 2002, http://robotics.caltech.edu/~stergios/tech_reports/tr_rpm_correl.pdf.

[17]   J. R. Wertz, Ed., *Spacecraft Attitude Determination and Control*, vol. 73 of *Astrophysics and Space Science Library*, D. Reidel Publishing Company, Dordrecht, The Netherlands, 1978.